Proceedings of the ASME 2012 11th Biennial Conference on Engineering Systems Design and Analysis
ESDA2012
July 2-4, 2012, Nantes, France

ESDA2012-82068

VERIFICATION OF A FINITE ELEMENT MODEL OF AN UNMANNED AERIAL VEHICLE WING TORQUE BOX VIA EXPERIMENTAL MODAL TESTING

Levent Unlusoy[2], Melin Sahin[1], and Yavuz Yaman
Department of Aerospace Engineering
Middle East Technical University
Ankara, TURKEY
[1]Contact Author
[2]Currently at University of Turkish Aeronautical Association, Faculty of Aeronautics and Astronautics, TURKEY

KEYWORDS
Unmanned Aerial Vehicle Wing, Ground Vibration Tests, Finite Element Modeling

ABSTRACT
In this study, the detailed finite element model (FEM) of an unmanned aerial vehicle wing torque box was verified by the experimental modal testing. During the computational studies the free-free boundary conditions were used and the natural frequencies and mode-shapes of the structure were obtained by using the MSC® Software. The results were then compared with the experimentally obtained resonance frequencies and mode-shapes. It was observed that the frequencies were in close agreement having an error within the range of 1.5-3.6%.

NOMENCLATURE

ACC	Accelerometer
FEA	Finite Element Analysis
FEM	Finite Element Model
FFT	Fast Fourier Transformation
FRF	Frequency Response Function
MPC	Multi Point Constraint
RBE	Rigid Body Element

INTRODUCTION
In this study, a detailed FEM of an unmanned aerial vehicle wing torque-box was generated and the structural analyses were conducted via finite element analysis (FEA). The inner components of the wing torque box were composed of two distinct materials, aluminum and fiber reinforced composite. The material used in the production of spars and the corner connectors was aluminum 7075-T651. The ribs were cut from sheet aluminum 2024-T3. The skin of the wing torque box, on the other hand, was manufactured with wet lay-up technique by using four layers of woven 7781 E-Glass fabric with a stacking sequence of 0°/45°/45°/0° having the matrix material as a combination of Araldite LY5052 resin and Aradur HY5052 hardener.

The detailed structural model of the wing was developed by using MSC® PATRAN and the theoretical dynamic analyses for natural frequencies and mode-shapes were conducted by using MSC® NASTRAN for free-free boundary conditions. After conducting theoretical analyses, a series of repeatable experiments were carried out on a manufactured full-scale wing torque-box and the results of the theoretical dynamic analyses were then compared with the obtained resonance frequencies. The roving-hammer test was used to get the frequency response data which was collected by using the FFT analyzer PULSE™. The obtained test data was then post-processed by using an in-house developed MATLAB code to extract the resonance frequencies and the corresponding mode-shapes of the wing torque-box. The information achieved through the comparisons made between FEA and modal test data was used for the model updating purposes in order to verify the mass and stiffness characteristics of the structural model of the torque box of the wing. The mentioned modal test data was used to detect the flexural and torsional vibrations due to the limitations in the experimental set-up hardware. Hence during the updating procedures the in-plane vibrations and their possible effects were currently omitted. After the relevant updating, it was determined that, in the frequency range of interest which covers the first and second flexural and first torsional modes, the results of FEA and the experiments were in close agreement within the envelope of 3.6% difference.

The wing studied here was actually installed on an unmanned aerial vehicle [4] and the vehicle was successfully flown.

THE GEOMETRICAL MODEL

The aim of the development of the geometrical model was to establish a satisfactory finite element model. The solid model was generated by using the package program MSC®PATRAN. The developed geometrical model is shown in Figure 1.

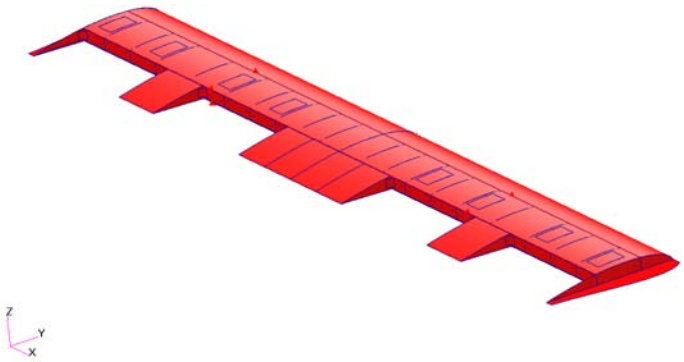

Figure 1 - Geometrical Model of the Wing Torque Box

THE FINITE ELEMENT MODEL

The detailed structural model of the wing torque box was developed by using MSC® PATRAN package program. The torque box contains four major structural parts: spars, ribs, skin and the connectors. These structural parts have very small thicknesses as compared to the other dimensions. Hence, they were preferred to be modeled as 2D shell elements in the finite element model. The flanges of the spars on the other hand, were modeled via 1D beam elements in order to get accurate flexural responses in dynamical analysis.

In real life application the composite skin was connected to the spars and ribs with rivets and resin. The combination of these two was assumed to be rigid connections, thus, they were modeled by using equivalence in the corresponding neighboring nodes on the ribs, spars and skin. On the other hand, the connections between the spars were done by specially designed connectors and rivets. These connections cannot be modeled as completely rigid connections. There should be some rotational freedom applied on these connections. The induced freedom on a rivet connection should simulate the rotation around the rivet itself for the case demonstrated in this study. However, the connection prevents the rotation around the rivet axis. Therefore, the mentioned degree of freedom cannot be set loose but must be limited with some level. That's the main reason of why MPC type elements were used for the modeling of the rivets in this study. The MPC elements make it possible to relate the deformation of the nodes to each other without the complete behavior set equivalent. The MPC elements provide fast and accurate solutions for linear deformations [1]. Hence in the current study, the rivets were modeled as RBE2 type MPC's at their exact geometrical location [2].

The developed finite element model is shown in Figure 2 and the elemental characteristics of the model are listed in Table 1. The spar cross-sections, the rib segments and a unique spar rib connection with the connector-rivet joints are shown in Figure 3, Figure 4 and Figure 5 respectively.

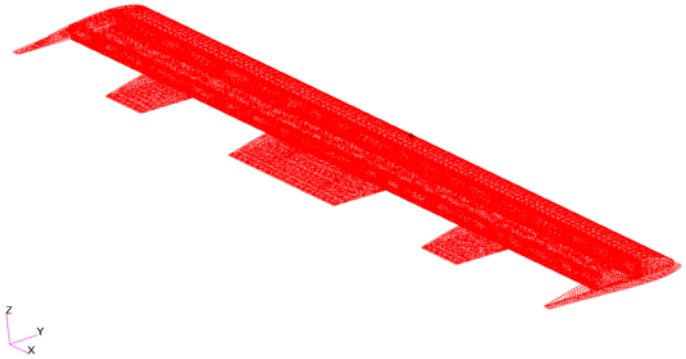

Figure 2 - Finite Element Model of the Wing Torque Box

Table 1 - Elemental Characteristics of the Finite Element Model

Element Type	Element Topology	Total Amount Used in FEM
1D Beam	Bar2	1200
2D Shell	Quad4	31652
2D Shell	Tria3	36
MPC	RBE2	213

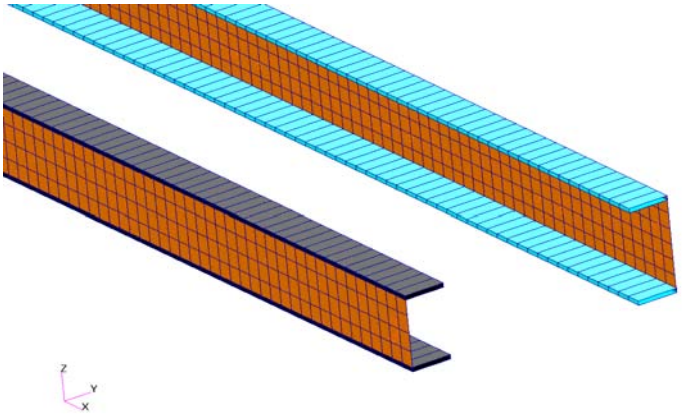

Figure 3 - Cross-sectional View of the Spars

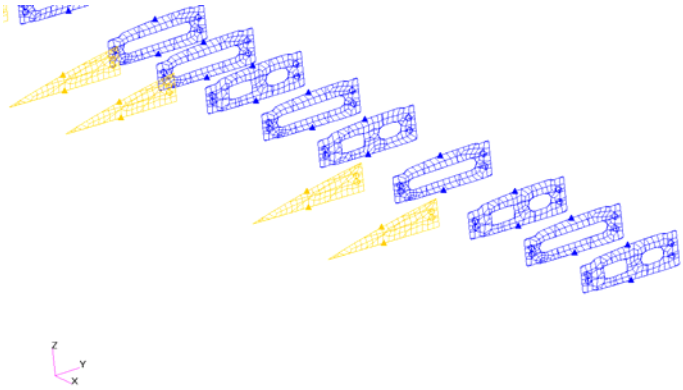

Figure 4 - The Ribs Used on the Right Half of the Wing Torque Box

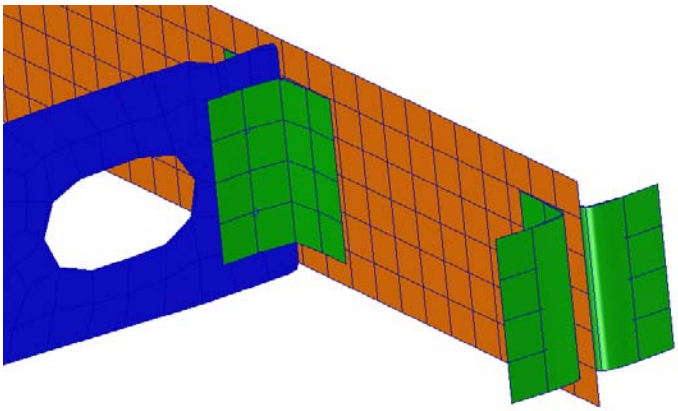

Figure 5 - A Unique Rib-Spar Connection via Connector-rivet Joints

THE FINITE ELEMENT ANALYSIS

The finite element analyses were conducted by using MSC® NASTRAN package program. The analyses were based on the natural frequencies and mode-shapes of the wing torque box. The boundary condition used in the analyses was Free-Free conditions [3]. By using the 103 solver of MSC® NASTRAN package program, the first three elastic modes were computed. The determined natural frequencies and the corresponding mode-shapes are tabulated in Table 2.

Table 2 - The Theoretical Natural Frequencies and Mode-Shapes of the Wing Torque Box

Mode-shape	Natural Frequency [Hz]
1st out-of-plane Bending	26.754
2nd out-of-plane Bending	73.556
1st Symmetric Torsion	83.242

The first three elastic mode-shapes are shown in Figure 6, Figure 7 and Figure 8 in ascending order of the natural frequencies.

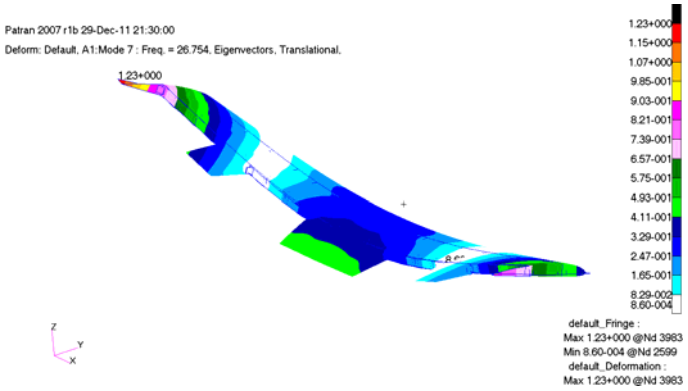

Figure 6 - First out-of-plane Bending Mode-shape at 26.754 [Hz]

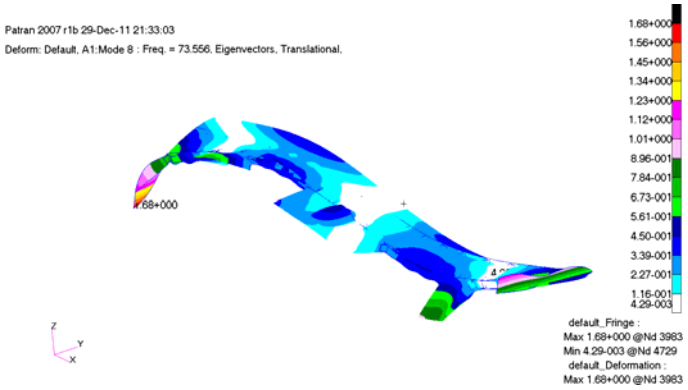

Figure 7 - Second out-of-plane Bending Mode-shape at 73.556 [Hz]

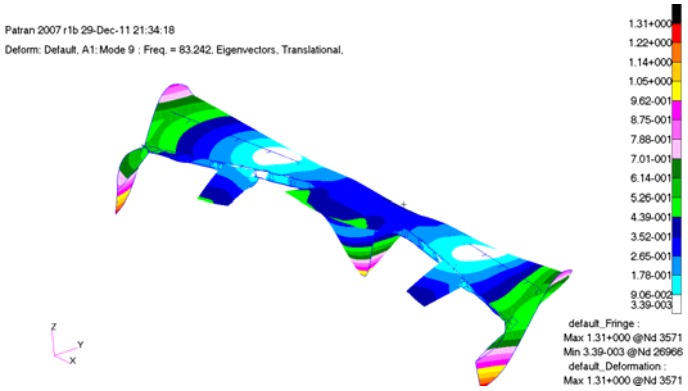

Figure 8 - First Symmetric Torsional Mode-shape at 83.242 [Hz]

EXPERIMENTAL MODAL TESTING

The experimental modal testing was conducted to verify the structural characteristics of the developed structural model of the unmanned aerial vehicle wing torque box. The analysis devices used in experimental setup during the modal testing is shown in Figure 9 and some of the equipment used were listed in Table 3.

Figure 9 - Analysis Equipment Used in the Experimental Setup [4]

Table 3 - The List of Equipment Used in the Experimental Modal Testing

Equipment	Type
FFT Analyzer	B&K Pulse 3560-C [5]
Power Amplifier	B&K 2720
Impact Hammer	B&K Type 8206 [6]
1-Axis Accelerometers	B&K Type 4508-B [7]

Free-Free boundary condition is not physically possible in the real life. In order to simulate the free-free boundary condition; the hanging of the structure from the ceiling or on another stiff structure is a known procedure [8]. In this experimental study, instead of soft springs, soft latex ropes were used. The wing torque box was hanged inside a steel frame with two latex ropes as shown in the Figure 10.

Figure 10 - Simulated Free-free Boundary Conditions in Laboratory

The methodology used in the experimental modal testing was roving hammer testing. Three single-axis accelerometers were attached on the wing. One was located at the middle on the front spar location (ACC2), one at the right tip of the wing on the rear spar location (ACC3) and the last one at the left tip of the wing on the leading edge (ACC1). This orientation made it possible to measure all three desired resonance frequencies and the corresponding mode-shapes.

The hammer excitation was used on 45 different data points mostly located on top of spars and ribs. Data collected from these points were pre-processed by the FFT Analyzer B&K Pulse 3560-C [5]. Then, the H2 data was bridged to MATLAB® and an in-house developed MATLAB® code was used for post processing. In the code developed the processed data was first averaged compositely for all three accelerometers. After that the averages of 45 measurements for each accelerometer were examined separately. Finally, the numerical value of the imaginary parts of the H2 data collected from each accelerometer at first three resonance frequencies were used in peak picking method in order to obtain the experimental mode-shapes [9, 10].

The total 135 data sets collected from three single-axis accelerometers all together are shown in Figure 11 and their unrated average is given in Figure 12.

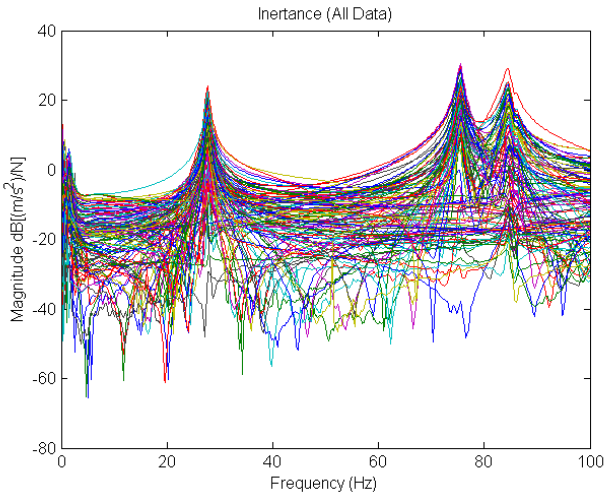

Figure 11 - All 135 H2 FRF Data Collected from Three Single-axis Accelerometers

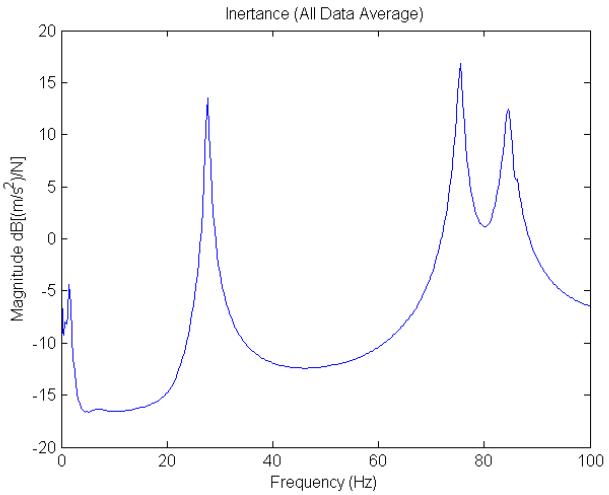

Figure 12 - The Unrated Average of All Data Collected from Three Single-axis Accelerometers

The average frequency response functions can also be shown for each accelerometer separately. The average of H2 FRF data collected at 45 measurements from ACC1, ACC2 and ACC3 are given respectively in Figure 13, Figure 14 and Figure 15.

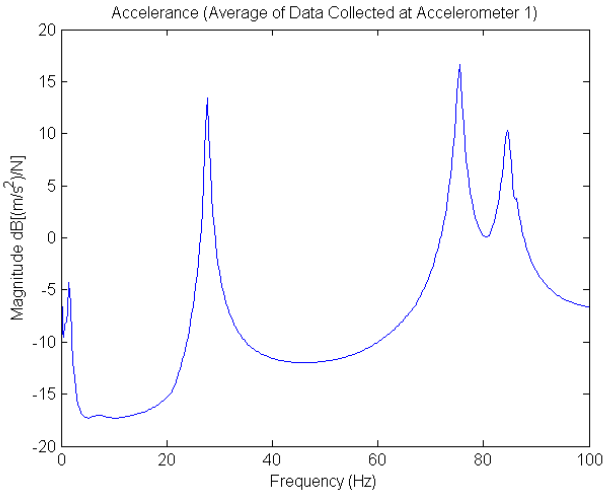

Figure 13 - The Average FRF of Data Collected by ACC1

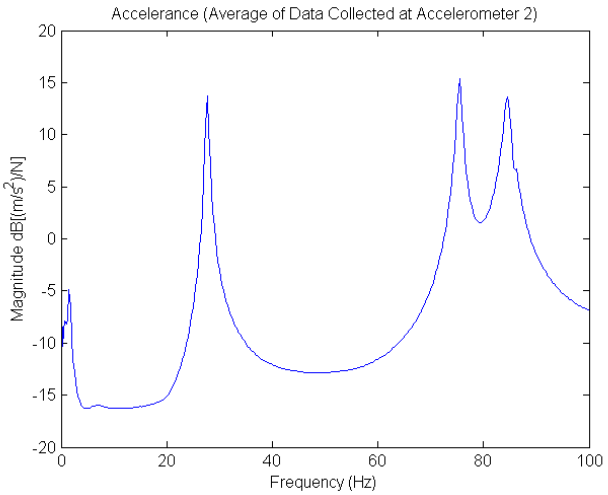

Figure 14 - The Average FRF of Data Collected by ACC2

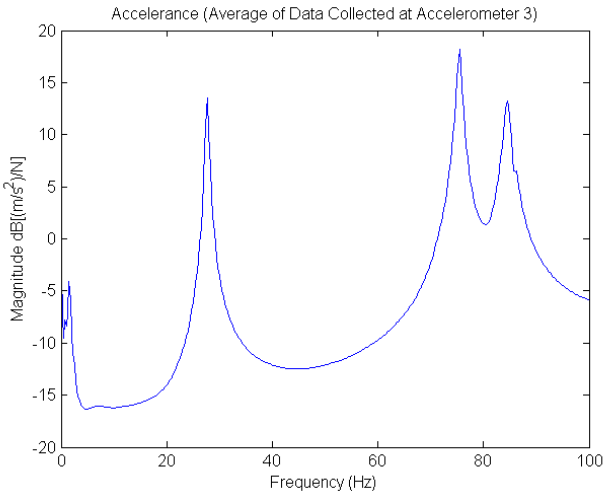

Figure 15 - The Average FRF of Data Collected by ACC3

As it can be clearly seen in the FRF figures there are 3 resonance frequencies within the range of 0-100 [Hz]. The corresponding values of resonance frequencies are 27.75 [Hz], 75.5 [Hz], 84.5 [Hz]. The experimental mode-shapes at these resonance frequencies were computed and are given in Figure 16, Figure 17 and Figure 18 in ascending order.

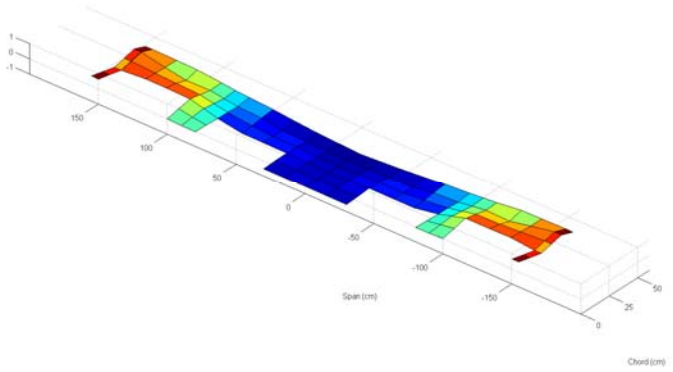

Figure 16 - Experimental Mode-shape at 27.75 [Hz]

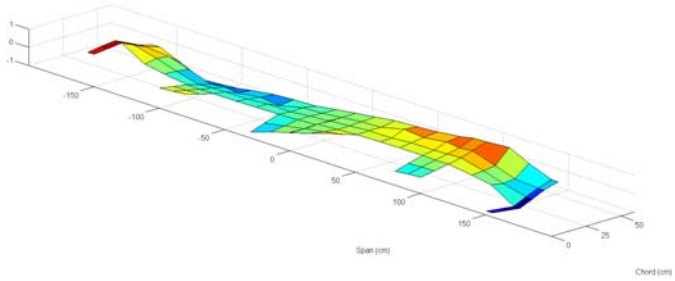

Figure 17 - Experimental Mode-shape at 75.5 [Hz]

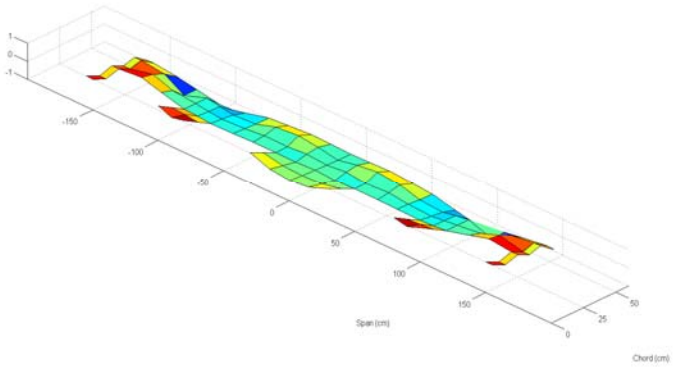

Figure 18 - Experimental Mode-shape at 84.5 [Hz]

Although, there were some unavoidable experimental errors due to the lack of coherence at repeated impact hammer hits, double hits and etc., the experimental mode-shapes were similar to the first and second out-of-plane bending and first symmetric torsional mode shapes respectively. The experimental results are summarized in tabular form in Table 4.

Table 4 - The Summary of the Resonance Frequency and Mode-shape Results Obtained by Experimental Model Testing

Mode-shape	Resonance Frequency [Hz]
1st out-of-plane Bending	27.75
2nd out-of-plane Bending	75.50
1st Symmetric Torsion	84.50

COMPARISON OF THE THEORETICAL AND THE EXPERIMENTAL DATA

The comparison between finite element analyses and experimental model testing results are given in Table 5.

Table 5 - Comparison of Experimental and Theoretical Results of Dynamic Characteristics of the Wing Torque Box

Mode-shape	Resonance Frequency [Hz.]	Natural Frequency [Hz.]	Percent Difference wrt Experiment
1st out-of-plane Bending	27.75	26.754	-3.6%
2nd out-of-plane Bending	75.50	73.556	-2.6%
1st Symmetric Torsion	84.50	83.242	-1,5%

The mode shapes for the natural/ resonance frequencies were found in close agreement. The maximum error in the magnitude of the natural/ resonance frequencies was determined to be 3.6%.

CONCLUSION

This study was based on the verification of the modelled dynamic characteristics of an unmanned aerial vehicle wing torque box via experimental modal testing. Throughout the study, a detailed finite element model of the wing torque box, including every rivet and bolt, was developed in MSC®PATRAN. Following the development of the FEM, the natural frequency and mode-shape analyses were conducted by using the solver 103 of MSC®NASTRAN. Then, an experimental procedure was designed, in which three fixed position single-axis accelerometer were used to collect the data from the roving hammer test established at 45 measurement points. The resulting 135 data set were then post processed in order to extract the FRF data and by peak picking method the mode-shapes corresponding to the resonance frequencies.

The comparison of the results had shown that the dynamic characteristics of the developed theoretical model and the manufactured actual wing were in close agreement within the envelope of 3.6% for the first three elastic global modes.

REFERENCES

[1] Naarayan, S. S., Kumar, D. V. T. G. P, Chandra, S., 2009, “Implication of Unequal Rivet Load Distribution in the Failures and Damage Tolerant Design of Metal and Composite Civil Aircraft Riveted Lap Joints”, Engineering Failure Analysis, Vol. 16, No. 7, pp.2255-2273

[2] Ünlüsoy L., 2010, “Structural Design and Analysis of a Mission Adaptive, Unmanned Aerial Vehicle Wing”, M.S. thesis, Middle East Technical University, ANKARA

[3] Blevins, R. D., 1979, “Formulas for Natural Frequency and Mode Shape”, Van Nostrand Reinhold Company, Inc., Florida, USA, Chap. 8

[4] Sahin M., Sakarya E., Unlusoy L., Insuyu E. T., Seber G., Ozgen S., Yaman Y., 2010, “Design, Analysis and Experimental Modal Testing of a Mission Adaptive Wing of an Unmanned Aerial Vehicle”, Paper No. 10, UVW2010, International Unmanned Vehicle Workshop, Turkish Air Force Academy, Istanbul, Turkey

[5] Product Data Sheet: Bruel& Kjaer 3560C Portable PULSE

[6] Product Data Sheet: Bruel&Kjaer 8206 Impact Hammer

[7] Product Data Sheet: Bruel&Kjaer 4508B Miniature DeltaTron Accelerometer

[8] Ewins, D. J., 1984, “Modal Testing: Theory and Practice”, Research Studies Press Ltd., Hertfordshire, England, Chap. 4-5

[9] Gade, S., Moller, S., Herlufsen, H., Konstantin-Hansen, H., 2006, “Frequency Domain Techniques for Operational Modal Analysis”, s08p06, *IMAC XXIV*, 2006

[10] Brincker, R., Zhang L., Andersen P., 2000, “Modal Identification from Ambient Responses using Frequency Domain Decomposition”, Proc. of the 18th International Modal Analysis Conference, San Antonio, Texas